Effect of Hydrolytic Degradation on the Microstructure of Poly(glycolic acid): An X-ray Scattering and Ultraviolet Spectrophotometry Study of Wet Samples Ultraviolet

E. KING, R. E. CAMERON

Department of Materials Science and Metallurgy, University of Cambridge, Cambridge, United Kingdom

Received 24 February 1997; accepted 20 April 1997

ABSTRACT: The effect of *in vitro* hydrolytic degradation on the microstructure of unoriented semicrystalline poly(glycolic acid) (PGA) was examined using simultaneous small- and wide-angle synchroton x-ray scattering (SAXS/WAXS) and ultraviolet (UV) spectrophotometry. Samples were degraded in buffer solutions at 37°C and were examined wet to avoid the structural changes that occur on drying. During degradation, the crystal density remained constant, and little change was seen in the lateral extent of the crystal lamellae. The transition layer between the crystalline and amorphous phases roughened slightly. More dramatic changes were seen in the amorphous phase, resulting in sharp increases in the crystallinity, the amount of glycolic acid in the buffer solution, and in the density difference between the crystal lamellae and the layers separating them. These changes indicated a loss of amorphous material that leveled off after 30 days. The lamellar repeat distance fell from around 95 to 80Å in the first 20 days before slowly rising again towards its initial value, changes which are interpreted as reflecting a two-stage loss of amorphous material, in which highly coiled loops and tie chains are degraded faster than taut tie chains. Once the coiled material is removed, the taut chains are able to adopt entropically favorable conformations, pulling the crystals towards each other, lowering the lamellar repeat, and creating internal stresses within the spherulite. As these newly coiled chains degrade, the crystals are released and slowly separate. The changes in long period are also considered in the light of chemical changes during degradation. Such change of chemical environment could affect the affinity for water of the amorphous inter-lamellar regions and affect the swelling. The observed changes in the long period may be a consequence of either or both of these factors.

These findings give microstructural information of importance in the prediction and control of mechanical properties during degradation and the diffusivity of other molecules through degrading PGA. © 1997 John Wiley & Sons, Inc. J Appl Polym Sci **66:** 1681–1690, 1997

Key words: hydrolytic degradation; poly(glycolic acid); lamellae; tie chains; crystallinity; wet

INTRODUCTION

Poly(hydroxy acid)s are an important class of biodegradable polymers for biomedical applications due to their biocompatibility and their physiologically tolerable degradation products. Poly(glycolic acid) (PGA) has been manufactured as a synthetic absorbable suture material, and its success has led to its development for other medical applications, such as implants, vascular grafts, artificial skin grafts, and drug release systems.[1]

PGA is the simplest linear aliphatic polyester.

Correspondence to: R. E. Cameron

Journal of Applied Polymer Science, Vol. 66, 1681–1690 (1997)
 CCC 0021-8995/97/091681-10

Because of the hydrophilic nature of the ester bond, it is hydrolytically degraded by body fluids. It is a semicrystalline thermoplastic with a high melting point of 224–227°C[2] and a glass transition temperature of around 37°C.[3] It has a very low solubility in most organic solvents,[4] which limits suitable processing techniques. The unit cell contains two molecular chains in planar zigzag conformation within an orthorhombic unit cell of dimensions $a = 5.22$Å, $b = 6.19$Å, and $c = 7.02$Å.[5] This article concerns the morphological changes that occur on degradation. These are of importance in understanding the associated changes in bulk properties, such as the ability of small molecules to diffuse through the polymer and the behavior under stress.

Chu and Campbell[6] performed a scanning electron microscopic study of the hydrolytic degradation of Dexon, a commercial synthetic suture material made up of colored braided PGA filaments. The material was degraded, then fully dried, before observation. They reported that the degradation of Dexon proceeds through two main stages. The amorphous region, being more accessible to the water, is attacked first, leading to loss of tensile strength within the fiber.[7] This is followed by the attack of the crystalline phase of the fiber microstructure. Ginde and Gupta[3] found significant differences between oriented and nonoriented samples. They monitored the sample mass, crystallinity, mechanical strength, and surface features, reporting a faster rate of degradation in PGA pellets than in fibers. In this study, pure PGA pellets and fibers were used, which were again studied fully dried. The crystallinity increased for both pellets and fibers, although the mass loss was greater in the pellets. They concluded that crystallinity and polymer chain orientation played an important role in the rate of degradation of PGA.

Fredericks et al.[8] studied the small-angle x-ray scattering (SAXS), wide-angle x-ray scattering (WAXS), density, infrared (IR) spectroscopy, and viscosity of the oriented suture material, Vicryl, a random copolymer containing 92 mol % glycolide units and 8 mol % lactide units during degradation. Again, the analysis was performed on the dried material. They found that the lamellar repeat and crystallite size parallel to the fiber axis decreased on degradation, and the crystallinity and density increased over the first 28 days. IR measurements gave evidence of the initial attack occurring in the amorphous area. They hypothesized that the chains at the interface of the crystallites and amorphous regions were preferentially degraded to the less accessible crystalline regions. We present a study of the effect of hydrolytic degradation on the microstructure of unoriented plates of PGA. In contrast to the studies reported above, the structures were studied wet, since significant changes are thought to occur on the removal of water.[9] Studying the changes occurring in the wet PGA microstructure thus allows closer association of the *in vitro* degradation results and the *in vivo* situation. Simultaneous small- and wide-angle synchrotron x-ray scattering, (SAXS/WAXS) analysis was used to determine the morphological changes, and ultraviolet (UV) spectrophotometry was used to measure the amount of glycolic acid, the degradation product of PGA, that evolved as degradation advanced.

EXPERIMENTAL

Materials

Pellets of PGA, with an inherent viscosity of 1.33 dL g, were obtained from Medisorb Technologies International, Cincinnati, Ohio. Plates 1×4 cm were formed by melting 0.8 g PGA at 230°C in a copper mold with a polytetrafluoroethylene (PTFE)-coated aluminium base, then crystallising at either 100 or 160°C. Phosphate-buffered saline solution, pH = 7.4, from (Sigma–Aldrich Company, Dorset, England) was made up with distilled water and with 1% penicillin–streptomycin antibiotic solution, from (Sigma–Aldrich Company). All apparatus was autoclaved for 30 minutes prior to use.

For the UV experiment, analytical grade chromotropic acid disodium salt and 96% sulphuric acid was obtained from (Fisher Scientific, Loughborough, England). 1.0 g of the acid disodium salt was dissolved in 250 mL sulphuric acid to make the chromotropic acid solution, used to produce a quantitative reaction with glycolic acid. Glycolic acid from Sigma–Aldrich Company was used to construct a calibration curve. Details of the preparation of the calibration curve are described by Chu and Louie.[10]

Degradation of PGA and UV Analysis

Plates of PGA were immersed in 50 ml buffer solution at 37°C. After a predetermined period of time, 1 ml of each solution was withdrawn and immediately mixed with 3 ml of the chromotropic acid

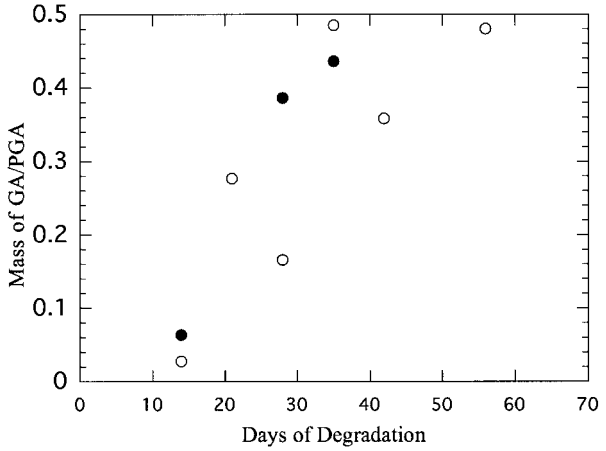

Figure 1 The ratio of the mass of glycolic acid in solution to the initial mass of poly(glycolic acid) placed in the solution for samples crystallised at 160°C (open circles) and 100°C (closed circles). The values were determined by UV titration of the buffer solution used to degrade the samples.

solution. The maximum absorbance was determined with a Shimadzu UV-visible spectrophotometer by scanning the solution from 200–900 nm. The calibration curve was used to determine the mass of glycolic acid in each solution. The ratio of the mass of glycolic acid to the mass of PGA originally placed in the solution was calculated for each degradation period.

Degradation of PGA and SAXS/WAXS

Plates of PGA were degraded as described above. After the predetermined period of time, the plates were removed from the buffer solution and immediately analyzed by simultaneous SAXS/WAXS. This was performed on beam line 8.2 at the SRS Laboratory at Daresbury, UK. The SRS laboratory allows data to be obtained over short exposure times due to the high intensity of the synchrotron radiation. Ryan et al. have described the experimental technique of SAXS/WAXS used to determine polymer structure.[11]

The WAXS data was obtained using a curved knife-edge detector, and the SAXS data was obtained using a quadrant detector located 3.5 m from the sample position. The SAXS detector was calibrated using wet collagen and the WAXS using high density polyethylene (HDPE). The wet samples were placed directly into the beam and exposed for 30 s. The SAXS data were divided by the detector response found by uniform illumination of the detector. Both WAXS and SAXS data were corrected for background scattering by subtracting the scattering from the straight through beam and for sample thickness and transmission by dividing by the signal from an ionisation chamber placed directly behind the sample.

RESULTS

UV Spectrophotometry

On combining the glycolic acid and buffer solution with the chromotropic acid solution, colors ranging from pale pink to deep purple developed, depending on the extent of degradation. The maximum wavelength absorbance was detected at 575 nm. The ratios of glycolic acid to PGA during degradation are shown in Figure 1. The concentration of glycolic acid increases on degradation.

SAXS Results

Figure 2 shows the SAXS data obtained for samples crystallised at 160°C. Similar results were obtained for the 100°C crystallised samples.

An attempt was made to model the data according to the two-phase model of Hoseman and Bagchi,[12,13] using modelling techniques described elsewhere.[14] However, it was not possible to obtain a satisfactory fit to the data with this model be-

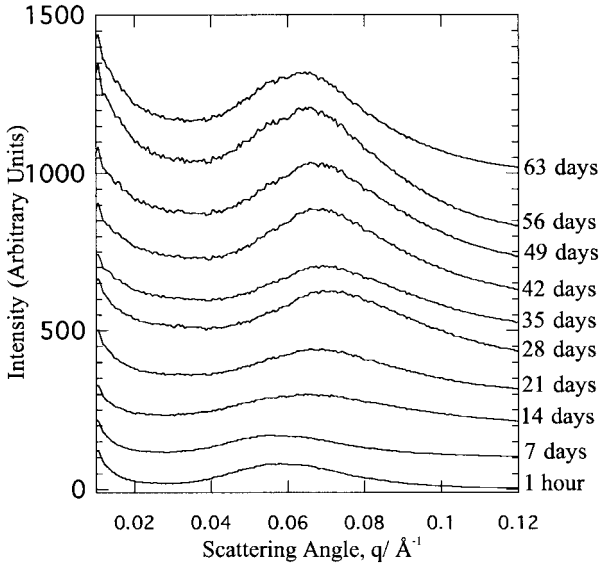

Figure 2 The SAXS intensity profiles for samples crystallised at 160°C and degraded for chosen times. The samples are observed without removal of buffer solution. Curves have been offset for clarity. The peak position shifts as degradation proceeds.

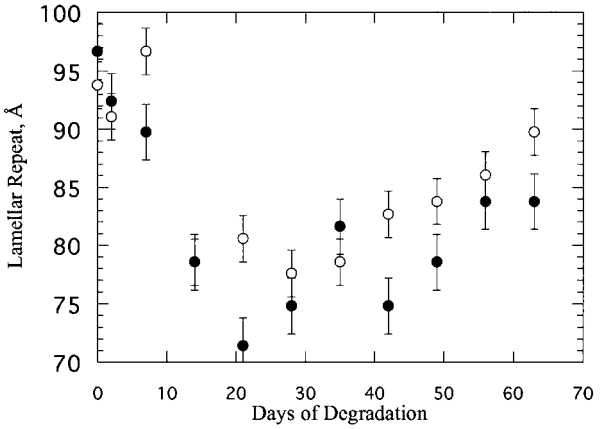

Figure 3 The lamellar repeat plotted against degradation time for samples crystallised at 160°C (open circles) and 100°C (closed circles). The values are obtained by applying the Bragg equation to the peak positions of the Lorentz corrected SAXS intensity profiles. In general, the repeat distance is higher for samples crystallised at 160°C.

cause the peaks in the data were too broad for any combination of parameters. A rough estimate of the repeat distance within the lamellar stack may be obtained by applying the Bragg equation to the Lorentz corrected peak positions. The Lorentz correction is applied by multiplying the intensity by the square of the scattering vector, thereby converting the data from randomly oriented lamellar stacks to that from a single lamellar stack. These repeat distance values are shown in Figure 3. Initially, the PGA has a lamellar repeat of approximately 95Å. Over the first 14 to 21 days of degradation, this distance falls to approximately 80Å, then slowly rises. The values for the samples crystallised at 160°C are consistently higher than those for the samples crystallised at 100°C.

The invariant of a SAXS profile,[15] Q, can be calculated using eq. (1).

$$Q = \frac{1}{2\pi^2}\int_0^\infty q^2 I(q)dq \qquad (1)$$

The invariant is unaffected by the shape of the scattering entities but dependant on the change in electron density differences within the structure.[16] Equation (2) gives the definition of Q for the pseudo two-phase structure illustrated in Figure 4.

$$Q = (\rho_c - \rho_a)^2\left[x_c(1 - x_c) - \frac{ES}{6V}\right] \qquad (2)$$

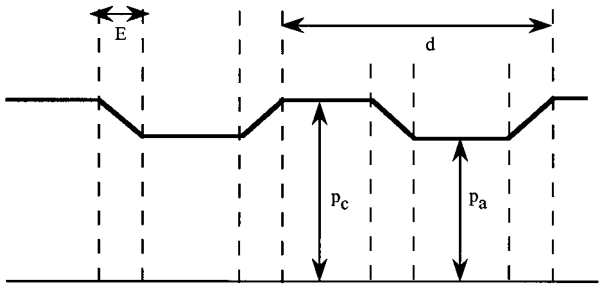

Figure 4 The electron density profile assumed in the interpretation of the invariant and the Porod analysis. The repeat distance d, the transition layer width E, the crystalline density ρ_c, and the amorphous density ρ_a are marked.

Where ρ_c is the density of the crystalline material, ρ_a is the density of the amorphous material, x_c is the crystallinity of the stack, E is the width of the transition layer between the amorphous and crystalline domains, and S/V is the phase boundary surface area per unit volume of polymer.

The invariant, calculated according to eq. (1), is shown against degradation time in Figure 5. The integration was performed between the limits of data collection. Since the intensities collected are in arbitrary units, the values obtained will differ from the true invariant by a constant factor, k.

Porod analysis[15] was performed by finding the gradient and intercept of Iq^2 versus q^{-2} in the high q region of the SAXS curve. From eq. (3), the values of the transition layer width, E and the Porod constant, Kp, can be determined. Equation (4) gives

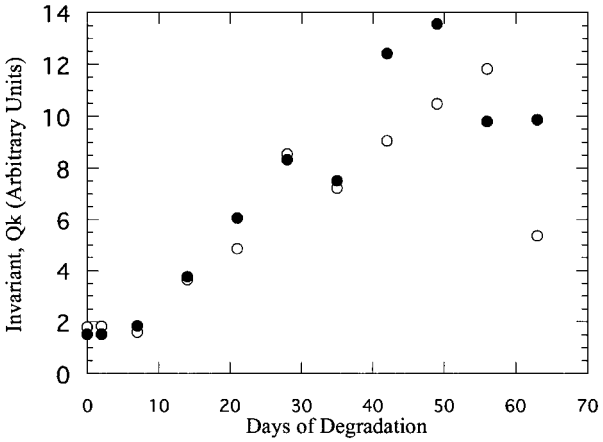

Figure 5 The invariant Q from the SAXS intensity profile, plotted against degradation time for samples crystallised at 160°C (open circles) and 100°C (closed circles). Since the intensity is given in arbitrary units, the invariant is also obtained in arbitrary units, related to standard units by an unknown constant k.

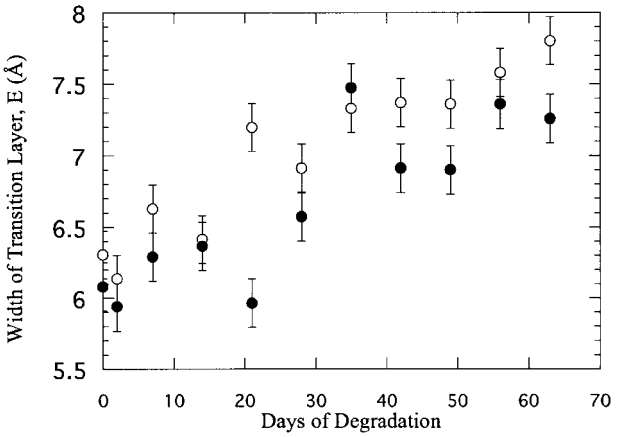

Figure 6 The width of the transition layer E plotted against degradation time for samples crystallised at 160°C (open circles) and 100°C (closed circles). These values are obtained from the Porod analysis described in the text.

the definition of the Porod constant in terms of parameters defined in eq. (2) and in Figure 4.

$$I(q) = \frac{16\mathrm{Kp}\pi^4}{q^4} - \frac{4\mathrm{Kp}E^2\pi^4}{3q^2} \tag{3}$$

$$Kp = \frac{\frac{S}{V}(\rho_c - \rho_a)^2}{8\pi^3} \tag{4}$$

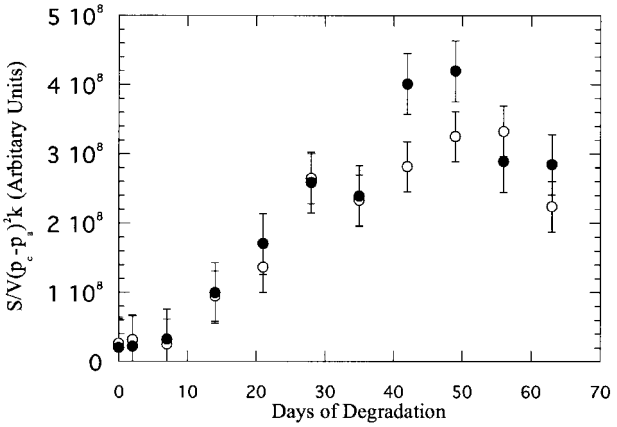

Figure 7 The surface to volume ratio multiplied by the density difference between crystalline and amorphous material squared plotted against degradation time for samples crystallised at 160°C (open circles) and 100°C (closed circles). These values are obtained by multiplying the Porod constant Kp by $8\pi^3$. Since the intensity is obtained in arbitrary units, the Porod constant is also in arbitrary units, related to standard units by an unknown constant k.

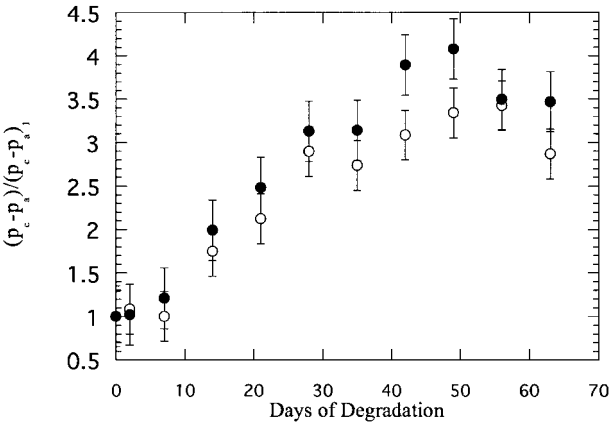

Figure 8 The density difference between crystalline and amorphous material divided by the value for samples degraded for one hour plotted against degradation time for samples crystallised at 160°C (open circles) and 100°C (closed circles). These values are derived from the repeat distance d and the Porod constant Kp, as described in the text.

On degradation, the width of the transition layer increases (Fig. 6), and the Porod constant increases. The Porod constant multiplied by $8\pi^3$ is shown in Figure 7. This, by eq. (4), is equivalent to the amount of surface area per unit volume of polymer combined with the change in density between the crystalline and amorphous phases, $(S/V)(\rho_c - \rho_a)^2$. Since the intensities collected are in arbitrary units, the values obtained will differ from the true value by the same constant factor, k, which multiplies the invariant.

An estimate of S/V may also be obtained from the repeat distance, d. By assuming that no new surface forms during the degradation, S/V can be approximated by eq. (5):

$$\frac{S}{V} = \frac{2}{d} \tag{5}$$

The change in density difference on degradation compared with the density difference after one-hour-degraded PGA was obtained by dividing $(S/V)(\rho_c - \rho_a)^2$ by $2/d$, as shown in eq. (6), where the subscript 1 denotes the value for the sample degraded for 1 hour.

$$\frac{(\rho_c - \rho_a)}{(\rho_c - \rho_a)_1} = \sqrt{\frac{\left[\left(\frac{S}{V}(\rho_c - \rho_a)^2 k\right) d/2\right]}{\left[\left(\frac{S}{V}(\rho_c - \rho_a)^2 k\right)_1 d_1/2\right]}} \tag{6}$$

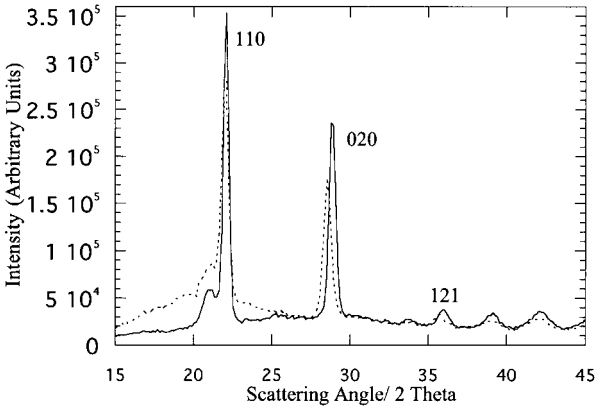

Figure 9 The WAXS intensity profiles for samples crystallised at 160°C and degraded for one hour (straight line) and degraded for 63 days (dashed line). The samples are observed without removal of buffer solution. Indices are given according to the orthorhombic unit cell proposed by Chantani et al.[5]

The constant k, which arises from arbitrary units of the intensity, thus cancels in this expression. An increase in this ratio was obtained up to 50 days degradation, then the value levelled (Fig. 8).

WAXS Results

Figure 9 shows the WAXS data obtained for samples crystallised at 160°C degraded for 1 hr and for 63 days. Similar results were obtained for the 100°C crystallised samples.

WAXS profiles were analyzed using the peak fitting program, "Fit," developed at the SRS, which fits curves to the crystal peaks and the amorphous halo. A Gaussian function fitted the peaks, and a third-order polynomial fit was found to be satisfactory for the amorphous halo. The positions of the 110, 020, and 121 peaks were used to calculate the dimensions of the unit cell. No major differences are seen on degradation, although the unit cell dimension along the b axis may decrease slightly, while a and c may show a slight increase (Fig. 10). No change in the overall crystal density was obtained (Fig. 11). The widths of the 110 and 020 peaks decreased slightly (Fig. 12).

The degree of crystallinity at the various stages of degradation was determined by finding the ratio of the area under the crystalline peaks to the total area under the WAXS pattern. An increase in crystallinity was observed levelling off after 30 days (Fig. 13).

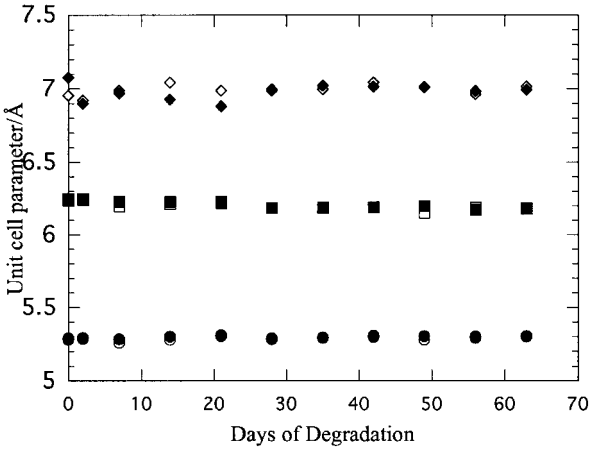

Figure 10 The unit cell parameters plotted against degradation time for samples crystallised at 160°C (open symbols) and 100°C (closed symbols). Parameters in the a direction are denoted by circles; in the b direction, by squares; and in the c direction, by diamonds.

DISCUSSION

The Effect of Starting Morphology

The samples crystallised at 160°C have a lamellar repeat 4 to 5Å higher than those crystallised at 100°C (Fig. 3). In general terms, this trend is to be expected since crystallisation at higher temperatures tends to result in a structure with fewer high-energy surfaces. For true isothermal crystallisation, however, the difference in lamellar repeat would be expected to be rather higher.[17] This suggests that significant crystallisation occurred

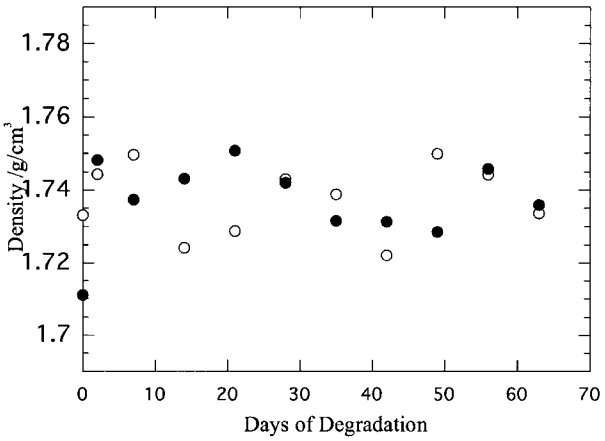

Figure 11 The crystal density plotted against degradation time for samples crystallised at 160°C (open circles) and 100°C (closed circles). These values were calculated from the orthorhombic unit cell parameters shown in Figure 10.

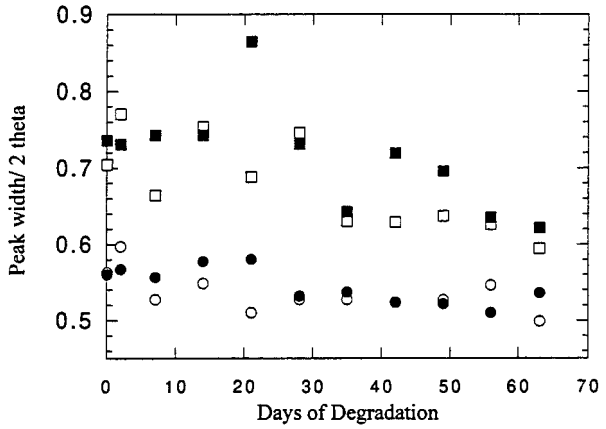

Figure 12 The widths of the wide-angle peaks plotted against degradation time for samples crystallised at 160°C (open symbols) and 100°C (closed symbols). Widths of the 110 peak are given by circles, and widths of the 020 peak are given by squares.

during the sample preparation as the polymer was cooled from the melt to the nominal crystallisation temperature, resulting in rather similar structures. The small differences in starting morphology do not appear to have affected the progress of degradation to within the uncertainties of measurement of the experiments reported here.

Minor changes in the crystalline phase

The unit cell parameters found from the WAXS peak positions (Fig. 10) are in reasonable agreement with values found by Chatani et al.[5] (a = 5.22Å, b = 6.19Å, and c = 7.02Å). The effect of degradation on the unit cell dimensions is small, although a slight decrease in size in the b direction (towards the value reported by Chatani et al.[5]) and a smaller opposing rise in the a and c directions are possible. Such changes could be an effect of changing constraints on the crystals as amorphous material is removed. The crystal density is unchanged by the degradation (Fig. 11).

The possible slight decrease in the widths of the WAXS peaks 110 and 020 (Fig. 12) may be interpreted via the Debye Scherrer equation[18] as an increased average lateral crystal size, perhaps because smaller crystals are fully lost more readily due to their large surface area, thereby increasing the average crystal size. This result may alternatively be interpreted as an increase in crystal perfection achieved as constraints are removed by the degradation of amorphous material, although no associated change is seen in the crystal density (Fig. 11). Whatever its cause, the effect is very small.

In conclusion, the changes to the unit cell and to the lateral extent of the crystals appear very small during the degradation performed.

Roughening of the Transition Layer

The width of the transition layer between crystalline and amorphous material increases slightly during the degradation (Fig. 6). This indicates a slight roughening of the crystal surfaces as the material degrades. This may be due to an uneven attack of fold surfaces of the crystal.

Preferential Degradation of Amorphous Material

The amount of glycolic acid released into the buffer solution increases with progressive degradation (Fig. 1). The scatter in these results is high, although it appears that the rate of increase slows after about 30 days, with the initial release presumably being a consequence of the relative easy degradation of the more accessible amorphous phase. Once this accessible material is removed, degradation continues more slowly as only more ordered and crystalline material remains.

The crystallinity as measured by WAXS increases with degradation from around 30 to about 50% (Fig. 13). Since the UV experiments suggest that a large amount of the polymer has been removed during this time, it must be assumed that the bulk of this is from the amorphous phase. As amorphous material is removed, the fraction of crystalline material in the remaining polymer in-

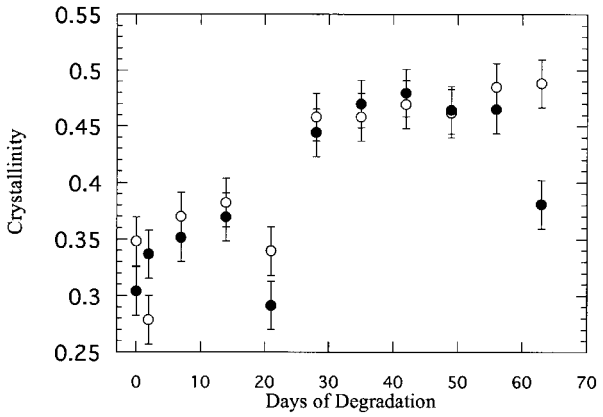

Figure 13 The crystallinity of the samples as calculated from the WAXS intensity profiles for samples crystallised at 160°C (open circles) and 100°C (closed circles).

creases. Again, the major change is seen over the first 30 days of degradation.

The loss of amorphous material and its replacement by buffer solution is also reflected in the increase in the density difference between amorphous and crystalline region (Fig. 8). The contrast, normalized to the contrast after one hour, increases steadily, levelling after about 30 to 50 days. As amorphous material is lost, the density of the layers between the crystals, ρ_a, falls. Since the crystal density is unchanged by the degradation (Fig. 11), the fall in ρ_a increases the density difference $(\rho_c - \rho_a)$. The levelling off occurs presumably when all the polymer in the layers between the crystal has been replaced by buffer solution. The ratio at this point is

$$\frac{\rho_c - \rho_b}{(\rho_c - \rho_a)_1} = \frac{1.74 - 0.98}{1.74 - (\rho_a)_1} \qquad (7)$$

where ρ_b is the density of the buffer solution (0.98 g cm^{-3}), and all values are given in g cm^{-3}. The density of the layers between crystals after 1 hour of degradation, $(\rho_a)_1$, may thus be calculated, yielding a value of 1.6 g cm^{-3}. This value appears very reasonable when compared with the relative values of crystalline and amorphous densities in other polymers.[19]

The invariant also increases on degradation (Fig. 5). This change is more difficult to interpret since the invariant is dependent on several changing parameters [eq. (2)]. The increase is likely to be dominated by the increase in the density difference between the crystals and the layers between them, $(\rho_c - \rho_a)$ via eq. (2). However, the invariant is also dependent on the crystallinity of the stack, the surface to volume ratio, and the interface thickness E, all of which are changing. The combined uncertainty of these measurements makes detailed interpretation of the invariant unproductive.

Thus, measurement of the release of glycolic acid, of the crystallinity, of the density difference, and of the invariant all indicate that amorphous material is degraded more quickly than the crystalline phase. The major loss seems to occur within the first 30 days of degradation.

Two-Stage Degradation of the Amorphous Phase

The changes in the lamellar repeat (Fig. 3) suggest that the loss of amorphous material may itself be a two-stage process. The lamellar repeat changes significantly during degradation. The greatest change is seen within the first 20 to 30 days of degradation when it falls by about 15Å. This is followed by a slow rise. By the end of the experiment, the initial value is almost regained.

The amorphous layers in PGA contain both loops and ties of amorphous PGA. Loops are formed by chains exiting a crystal surface and reentering the same crystal at a chosen point. Tie chains connect two adjacent crystalline lamellae. Most tie chains will be highly coiled, maximizing entropy. However, a minority will be pulled tightly by the entropic forces of the other amorphous chains [Fig. 14(a)].[20] The conformation of a chain is likely to affect its reactivity. Such effects on reactivity have been observed in the oxidation of polyolefins, although with contradictory conclusions. Some authors report[21,22] that the highly coiled amorphous material is more reactive than the conformationally strained extended tie chains and will degrade first. Others[23] suggest that strained chains are more susceptible to oxidation, implying the taut chains will be attacked before the coiled amorphous material.

If the coiled amorphous material is removed first,[21,22] an explanation may be offered for the effects seen in the lamellar repeat on degradation (Fig. 3). The taut tie chains are able to relax into more entropically favorable conformations, pulling the crystals closer together and lowering the lamellar repeat [Fig. 14(b)]. This proposed mechanism would explain the drop in the lamellar repeat observed in PGA. The crystals will have gained mobility following the loss of the majority of the amorphous material.

The wet samples do not appear to decrease in size with degradation, despite the removal of amorphous material and the collapse of the lamellae. The entropic driving force for the drop in lamellar repeat will be opposed by the spherulitic crystal architecture, despite an enhanced mobility of the crystal layers, since a narrowing of the gap between crystals in some areas will necessarily create stresses and perhaps voids in other areas. [In these wet samples, there is little evidence for voiding in the SAXS intensity profile (Fig. 2)], although partially degraded samples show a strong tendency to void if dried.[9] Voids too large to be visible in the SAXS profile may of course be present (the PGA becomes brittle with signs of surface cracks on degradation). The remaining tie chains are thus unlikely to reach their state of maximum entropy; and the lamellar repeat with arise from a balance between the entropic forces in the tie chain, encouraging contraction, and

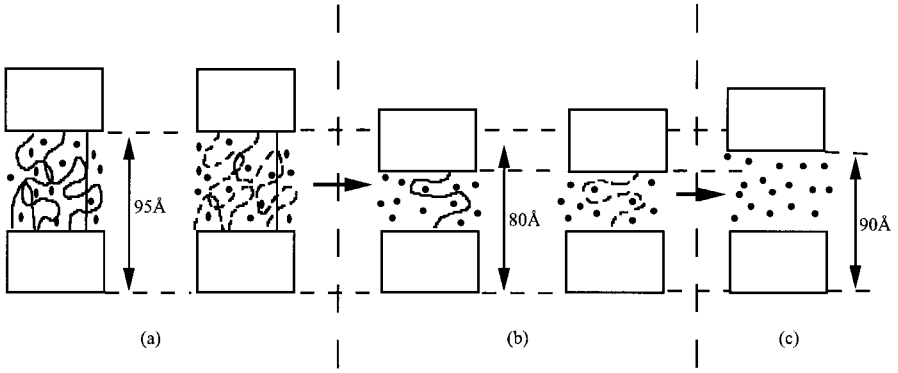

Figure 14 Schematic diagram of the changes that occur to the lamellar morphology of poly(glycolic acid) on degradation. (a) During days 0 to 20, highly coiled tie chains and loops are removed, leaving taut tie chains undegraded. (b) From day 20, taut tie chains are now able to coil under entropy drawing the crystals closer together. The crystals are mobile following the removal of the bulk of the amorphous material. However, the movement is likely to cause stresses elsewhere in the spherulite. Since the remaining tie chains are now coiled, they are reactive and will be able to degrade. (c) From day 20, the removal of the remaining tie chains leaves the crystals free to separate under the influence of the stresses elsewhere in the spherulite.

stresses in the spherulitic architecture, encouraging expansion.

As the tie chains relax, they become more reactive and degrade. The forces pulling the crystals together are thereby released, and the lamellar repeat slowly rises again [Fig. 14(c)].

Thus, the loss of amorphous material may occur via two stages. Reactive highly coiled chains are degraded over the first 20 days. This allows tight tie chains to relax to more entropically favourable conformations, pulling the crystals closer together and creating stresses elsewhere in the structure. Such stresses lead to voids if the structure if dried out. The newly coiled tie chains are now progressively degraded, partially releasing the crystals and allowing lamellar repeat to expand towards its initial value. Once all the accessible amorphous material is removed, degradation proceeds more slowly as only the more ordered and crystalline material remains.

Changes in affinity for water

As the polymer degrades, the chemical environment in the inter-lamellar regions changes. This may well affect the affinity for the water in these regions, altering the ability of the material to swell. The changes in the long period could therefore be a consequence of a changing affinity of the amorphous layers for water during degradation.

The concepts of a two stage removal of amorphous material and of changes in affinity for water are not mutually exclusive. It is possible that either or both control the total lamellar repeat.

The Consequences for Bulk Properties and for Applications of the Polymer

The loss of the amorphous material, the changing character of the connecting tie chains, and spherulitic stresses will have significant effects on the mechanical properties of PGA. A rapid loss of tensile strength and an increase in crystallinity in dry degraded PGA is reported.[7] These greatly affect the potential employment of PGA for further surgical applications where the controlled mechanical performance is essential.

As degradation proceeds, the ability of other molecules to diffuse into and out of the polymer will be significantly affected. The layers between the crystals, which provide natural channels for diffusion, change in character as material is removed; and the remaining chains change conformation and in size. This will affect the ability of biological molecules to diffuse from the body into a PGA implant. Similarly, the diffusion of an embedded drug out of a continuous PGA matrix controlled release system would be strongly affected by the changes described. Prediction and control of drug release is likely to depend on a knowledge of these changes.

The microstructural changes reported are intimately connected to the semi-crystalline morphology of the polymer. Although the processing

routes used here did not produce significantly different starting structures, careful control of crystallisation temperature or quenching, followed by post-annealing at chosen temperatures, could result in large variation in the starting morphology. Structures are possible that differ widely in their lamellar repeat. This would result in differences in the nature and proportion of tie chains[24,25] and in the size and separation of crystals. Such changes may well affect the balance of forces in the morphology during degradation, affecting the structure's response to degradation and perhaps affecting the structure's tendency to void. Significant effects on the size and nature of channels available for diffusion, as well as mechanical properties, would result.[26]

CONCLUSIONS

Although the results presented here are broadly in agreement with the previously reported model of microstructural change in PGA fibers, in that the amorphous material is seen to degrade faster than the crystalline material, they allow a more detailed description of morphological changes on degradation to be proposed.

During degradation, the crystal density remains constant, and little change is seen in the lateral extent of the crystal lamellae. The transition layer between the crystalline and amorphous phases roughens slightly. A sharp increase is seen in the crystallinity, the amount of glycolic acid in the buffer solution, and in the density difference between the crystal lamellae and the layers separating them. These changes indicate major loss of amorphous material within the first 30 days of degradation. Changes in the lamellar repeat distance are interpreted as reflecting a two-stage loss of amorphous material, in which highly coiled loops and tie chains are degraded faster than taut tie chains. Once the coiled material is removed, the taut chains are able to adopt entropically favorable conformations, lowering the lamellar repeat and creating internal stresses within the spherulite. As these newly coiled chains degrade, the crystals are released and slowly separate.

These findings give microstructural information of importance in the prediction and control of mechanical properties during degradation and the diffusivity of other molecules through degrading polymer.

The authors are grateful to Pfizer Central Research and the EPSRC for financial support. The X-ray experiments were performed at the CCLRC Daresbury Laboratory with the help and advice of Dr. B. U. Komanschek.

REFERENCES

1. X. Zhang, F. A. Goosen, U. P. Wyss, and D. Pichora, *Rev. Macromol. Chem. Phys.,* **C33,** 81 (1993).
2. C. C. Chu, *J. Biomed. Mater. Res.,* **15,** 19 (1981).
3. R. M. Ginde and R. K. Gupta, *J. Appl. Polym. Sci.,* **33,** 2411 (1987).
4. I. Engelberg and J. Kohn, *Biomat.,* **12,** 292 (1991).
5. Y. Chatani, K. Suehiro, Y. Okita, H. Tadokoro, and K. Chujo, *Makromol. Chem.,* **113,** 215 (1968).
6. C. C. Chu and N. D. Campbell, *J. Biomed. Mater. Res.,* **16,** 417 (1982).
7. C. C. Chu, *J. Appl. Polym. Sci.,* **26,** 1727 (1981).
8. R. J. Fredericks, A. L. Melveger, and L. J. Dolegiewitz, *J. Polym. Sci., Polym. Phys. Ed.,* **22,** 57 (1984).
9. E. King and R. E. Cameron, submitted to J. Macromol. Sci., Part A.
10. C. C. Chu and M. Louie, *J. Appl. Polym. Sci.,* **30,** 3133 (1985).
11. A. J. Ryan, S. Naylor, B. Komanschek, W. Bras, G. R. Mant, and G. E. Derbyshire, ACS Symposium Series 581. Hyphenated Techniques in Polymer Characterization. Thermal-spectroscopic and other methods, T. Provder, M. W. Urban, and H. G. Barth, Eds., American Chemical Society, Washington, D.C. 1994.
12. R. Hoseman and S. N. Bagchi, *Direct Analysis of Diffraction by Matter,* North Holland, Amsterdam, 1962.
13. R. Hoseman, *Z. Phys.,* **128,** 465 (1950).
14. B. L. Hurrell and R. E. Cameron, to appear.
15. F. J. Balta-Calleja and C. G. Vonk, *Polymer Science Library 8: X-ray Scattering of Synthetic Polymers,* Elsevier, Oxford, 1989.
16. O. Glatter and O. Kratky, *Small Angle X-ray Scattering,* Academic Press, London, 1982.
17. R. J. Young and P. A. Lovell, *Introduction to Polymers,* 2nd ed., Chapman & Hall, London, 1991.
18. B. D. Cullity, *Elements of X-ray Diffraction,* Addison-Wesley, London, 1956.
19. I. M. Campbell, *Introduction to Synthetic Polymers,* Oxford Science Publications, Oxford, 1994.
20. V. A. Behrstein and V. M. Egorov, *Differential Scanning Calorimetry of Polymers,* Ellis Horwood, London, 1994.
21. N. Ya. Rapoport, A. Sh. Goniashvili, M. S. Akutin, and V. B. Miller, *Vysokomol. Soyed.,* **A19,** 2211 (1977).
22. L. S. Shibryaeva, S. G. Kiryushkin, and G. E. Zaikov, *Int. J. Polym. Mater.,* **16,** 71 (1992).
23. J. Schiers, S. W. Bigger, and O. Delatycki, *J. Polym. Sci., Polym. Phys. Ed.,* **29,** 795 (1991).
24. Y. L. Huang and N. Brown, *J. Polym. Sci., Polym. Phys. Ed.,* **29,** 129 (1991).
25. C. M. Guttman, E. A. DiMarzio, and J. D. Hoffmann, *Polymer,* **22,** 1466 (1981).
26. C. C. Chu and A. Browning, *J. Biomed. Mat. Res.,* **22,** 699 (1988).